

UDC: 538.9 Condensed matter Physics, Solid state Physics, Theoretical Condensed matter Physics

## FOURTH ORDER PERTURBED HEISENBERG HAMILTONIAN OF FCC STRUCTURED FERROMAGNETIC ULTRA-THIN FILMS

P. Samarasekara<sup>1</sup> and E.M.P. Ekanayake<sup>2</sup>

<sup>1</sup>Department of Physics, University of Peradeniya, Peradeniya, Sri Lanka

<sup>2</sup>Department of Mathematical Sciences, Wayamba University of Sri Lanka, Kuliyaipitiya, Sri Lanka.

**Abstract:** *For the first time, fcc structured ferromagnetic thin films with two spin layers are described using fourth order perturbed Heisenberg Hamiltonian. Magnetic energy per unit spin was expressed in terms of spin exchange interaction and second order anisotropy constants in two spin layers. All the peaks are closely packed in the graphs plotted using fourth order perturbed Heisenberg Hamiltonian compared to peaks in the graphs plotted using third order perturbed Heisenberg Hamiltonian. 3-D plots of energy versus angle and each energy parameter were plotted. Peaks are periodically distributed only in the 3-D graph of energy versus angle and second order anisotropy constant of top spin layer. The magnetic energy increases when the value of second order anisotropy constant in bottom spin layer increases. In addition, the magnetic energy does not change considerably when the values of second order anisotropy constants of two spin layers are interchanged.*

**Keywords:** *Heisenberg Hamiltonian, fourth order perturbation, magnetic thin films, spin*

### 1. Introduction:

Although magnetic properties of thin films have been previously described using second and third order perturbed Heisenberg Hamiltonian, Heisenberg Hamiltonian has never been developed up to fourth order perturbation. Not only Heisenberg Hamiltonian, but also some other models have been applied to explain magnetic properties of thin films. Ferromagnetic films find potential applications in magnetic memory devices and microwave devices. Magnetic thin films are employed in miniature magnetic devices. Magnetic easy axis oriented films provide the same magnetic properties as bulk magnetic materials. Energy density of magnetic easy axis oriented films is almost same as that of bulk magnetic materials. However, the detailed theoretical studies related to the easy axis orientation are limited. The quasistatic magnetic hysteresis of ferromagnetic thin films grown on a vicinal substrate has been theoretically explored using Monte Carlo simulations [1]. Structural and magnetic properties of two dimensional FeCo ordered alloys have been investigated by first principles band structure theory [2]. EuTe films with surface elastic stresses have been theoretically studied using Heisenberg Hamiltonian [3]. De Vries theory was employed to explain the magnetostriction of dc magnetron sputtered FeTaN thin films [4]. Magnetic layers of Ni on Cu have been theoretically investigated using the Korringa-Kohn-Rostoker Green's function method [5]. Electric and magnetic properties of multiferroic thin films have been theoretically described using modified Heisenberg model and transverse Ising model coupled with Green's function technique [6].

The interfacial coupling dependence of the magnetic ordering in ferro-antiferromagnetic bilayers has been studied using the Heisenberg Hamiltonian [7]. Heisenberg Hamiltonian incorporated with spin exchange interaction, magnetic dipole interaction, applied magnetic field, second and fourth order magnetic anisotropy terms has been solved for ferromagnetic thin films [8, 9, 10]. The domain structure and Magnetization reversal in thin magnetic films was described using computer

simulations [11]. Heisenberg Hamiltonian has been employed to theoretically describe in-plane dipole coupling anisotropy of a square ferromagnetic Heisenberg monolayer [12]. Previously magnetic thin films have been fabricated using sputtering and pulse laser deposition techniques by us [13-15]. According to our experimental studies, some magnetic energy parameters were found to be important in the control of magnetic easy axis orientation. Ferrite films have been explained using second order perturbed Heisenberg Hamiltonian by us [16, 17]. In addition, Heisenberg Hamiltonian was employed to describe the variation of magnetic easy axis orientation of experimentally deposited magnetic thin films with temperature [18-20]. Second and third order perturbed Heisenberg Hamiltonian was applied to explain the ferromagnetic films by us [21, 22]. Unperturbed Heisenberg Hamiltonian was applied to describe ferrite thin films [23]. Magnetic properties of ferrite films have been elucidated using and third order perturbed Heisenberg Hamiltonian by us [24]. Magnetostatic energy of domains and domain walls has been theoretically investigated as a function of film thickness [25]. Magnetic thin films with thicknesses ranging from 2 to 4 layers have been modeled using anisotropic classical Heisenberg spins under the influence of mechanical uniaxial stresses [26]. Monte carlo simulation has been employed to study magnetic properties of very thin films with bcc lattice [27]. The properties of thin films made of stacked triangular layers of atoms bearing Heisenberg spins with an Ising like interaction anisotropy have been investigated using extensive Monte Carlo simulations and analytical Green's function [28]. A Green's function technique is applied for the Heisenberg model to study the influence of the magnetic surface single ion anisotropy on the spin wave spectrum including damping effects in ferromagnetic thin films [29].

## 2. Model:

Classical Heisenberg Hamiltonian of ferromagnetic thin films with spin exchange interaction, long range dipole interaction and second order magnetic anisotropy can be conveyed as [16-24].

$$H = -\frac{J}{2} \sum_{m,n} \vec{S}_m \cdot \vec{S}_n + \frac{\omega}{2} \sum_{m \neq n} \left( \frac{\vec{S}_m \cdot \vec{S}_n}{r_{mn}^3} - \frac{3(\vec{S}_m \cdot \vec{r}_{mn})(\vec{r}_{mn} \cdot \vec{S}_n)}{r_{mn}^5} \right) - \sum_m D_{\lambda_m}^{(2)} (S_m^z)^2 \quad (1)$$

After taking the dot products of vectors, this equation can be deduced to following form for a unit spin [16-24]

$$E(\theta) = -\frac{1}{2} \sum_{m,n=1}^N [(JZ_{|m-n|} - \frac{\omega}{4} \Phi_{|m-n|}) \cos(\theta_m - \theta_n) - \frac{3\omega}{4} \Phi_{|m-n|} \cos(\theta_m + \theta_n)] - \sum_{m=1}^N D_m^{(2)} \cos^2 \theta_m \quad (2)$$

Where  $m$  and  $n$  indicate indices of two different spin layers,  $N$  exhibits the number of layers measured in direction perpendicular to the film plane,  $J$  is the magnetic spin exchange interaction,  $Z_{|m-n|}$  stands for the number of nearest spin neighbors,  $\omega$  represents the strength of long range dipole interaction,  $\Phi_{|m-n|}$  are constants for partial summation of dipole interaction, For non-oriented films, above angles  $\theta_m$  and  $\theta_n$  measured with film normal can be expressed in forms of  $\theta_m = \theta + \varepsilon_m$  and  $\theta_n = \theta + \varepsilon_n$ , and cosine and sine terms can be expanded up to the fourth order of  $\varepsilon$  as following. For a ferromagnetic thin film with only two spin layers,  $N$  changes from 1 to 2.

$$E(\theta)=E_0+E(\varepsilon)+E(\varepsilon^2)+E(\varepsilon^3)+E(\varepsilon^4)$$

(3)

Here

$$E_0 = -JZ_0 + \frac{\omega\phi_0}{4} - JZ_1 + \frac{\omega\phi_1}{4} + \frac{3\omega}{8}(2\phi_0 + 2\phi_1)\cos 2\theta - D_1^{(2)} \cos^2 \theta - D_2^{(2)} \cos^2 \theta$$

$$E(\varepsilon) = -\frac{3\omega}{4}[(\phi_0 + \phi_1)(\varepsilon_1 + \varepsilon_2)]\sin 2\theta + 2\cos\theta\sin\theta(D_1^{(2)}\varepsilon_1 + D_2^{(2)}\varepsilon_2)$$

$$E(\varepsilon^2) = \left( JZ_1 - \frac{\omega\phi_1}{4} \right) \left( \frac{\varepsilon_1^2 + \varepsilon_2^2 - 2\varepsilon_1\varepsilon_2}{2} \right) - \frac{3\omega}{8}\cos 2\theta(2\phi_0(\varepsilon_1^2 + \varepsilon_2^2) + (\varepsilon_1^2 + \varepsilon_2^2 + 2\varepsilon_1\varepsilon_2)\phi_1) + \varepsilon_1^2(D_1^{(2)}\cos^2\theta - D_1^{(2)}\sin^2\theta) + \varepsilon_2^2(D_2^{(2)}\cos^2\theta - D_2^{(2)}\sin^2\theta)$$

$$E(\varepsilon^3) = \frac{\omega}{8}(4\phi_0(\varepsilon_1^3 + \varepsilon_2^3) + \phi_1(\varepsilon_1^3 + 3\varepsilon_1\varepsilon_2^2 + 3\varepsilon_1^2\varepsilon_2 + \varepsilon_2^3))\sin 2\theta - \frac{4\cos\theta\sin\theta}{3}(D_1^{(2)}\varepsilon_1^3 + D_2^{(2)}\varepsilon_2^3)$$

$$E(\varepsilon^4) = -\left( JZ_1 - \frac{\omega\phi_1}{4} \right) \left( \frac{\varepsilon_1^4 + \varepsilon_2^4 + 6\varepsilon_1^2\varepsilon_2^2 - 4\varepsilon_1^3\varepsilon_2 - 4\varepsilon_1\varepsilon_2^3}{24} \right) + \frac{\omega}{8} \left[ 2\phi_0(\varepsilon_1^4 + \varepsilon_2^4) + \phi_1 \left( \frac{\varepsilon_1^4 + \varepsilon_2^4 + 6\varepsilon_1^2\varepsilon_2^2 + 4\varepsilon_1^3\varepsilon_2 + 4\varepsilon_1\varepsilon_2^3}{4} \right) \right] \cos 2\theta - \varepsilon_1^4 \left( \frac{D_1^{(2)}\cos^2\theta}{3} - \frac{D_1^{(2)}\sin^2\theta}{3} \right) - \varepsilon_2^4 \left( \frac{D_2^{(2)}\cos^2\theta}{3} - \frac{D_2^{(2)}\sin^2\theta}{3} \right)$$

First order perturbation term can be expressed in terms of a row and a column matrices with two terms in each as following.

$$E(\varepsilon)=\vec{\alpha}\cdot\vec{\varepsilon}$$

Here terms of  $\alpha$  are given by  $\alpha_1 = -\frac{3\omega}{4}(\phi_0 + \phi_1)\sin 2\theta + 2\cos\theta\sin\theta D_1^{(2)}$

$$\alpha_2 = -\frac{3\omega}{4}(\phi_0 + \phi_1)\sin 2\theta + 2\cos\theta\sin\theta D_2^{(2)}$$

Second order perturbation term can be rendered in terms of a two by two matrix, a row matrix and a column matrix as following.

$$E(\varepsilon^2) = \frac{1}{2} \vec{\varepsilon} \cdot C \cdot \vec{\varepsilon}$$

Elements of 2x2 matrix ( $C$ ) are delineated by

$$C_{11} = JZ_1 - \frac{\omega\phi_1}{4} - \frac{3\omega}{4}(2\phi_0 + \phi_1)\cos 2\theta + 2(D_1^{(2)}\cos^2\theta - D_1^{(2)}\sin^2\theta)$$

$$C_{22} = JZ_1 - \frac{\omega\phi_1}{4} - \frac{3\omega}{4}(2\phi_0 + \phi_1)\cos 2\theta + 2(D_2^{(2)}\cos^2\theta - D_2^{(2)}\sin^2\theta)$$

$$C_{12} = C_{21} = -JZ_1 + \frac{\omega\phi_1}{4} - \frac{3\omega\phi_1}{4}\cos 2\theta$$

Third order perturbation can be expressed in terms of a two by two matrix, a row matrix and a column matrix as following.

$$E(\varepsilon^3) = \varepsilon^2 \beta \cdot \vec{\varepsilon}$$

Elements of two by two matrix ( $\beta$ ) are specified by

$$\beta_{11} = \frac{\omega}{8}(4\phi_0 + \phi_1)\sin 2\theta - \frac{4D_1^{(2)}\cos\theta\sin\theta}{3}$$

$$\beta_{22} = \frac{\omega}{8}(4\phi_0 + \phi_1)\sin 2\theta - \frac{4D_2^{(2)}\cos\theta\sin\theta}{3}$$

$$\beta_{12} = \beta_{21} = \frac{3\omega}{8}\phi_1\sin 2\theta$$

Fourth order perturbation can be rendered in terms of two by two matrices, row matrices and column matrices as following.

$$E(\varepsilon^4) = \varepsilon^3 F \cdot \vec{\varepsilon} + \varepsilon^2 G \varepsilon^2$$

Elements of two by two matrices ( $F$  and  $G$ ) are delineated by

$$F_{11} = -\frac{1}{24}\left(JZ_1 - \frac{\omega\phi_1}{4}\right) + \frac{\omega}{8}\left(2\phi_0 + \frac{\phi_1}{4}\right)\cos 2\theta - \frac{D_1^{(2)}\cos^2\theta}{3} + \frac{D_1^{(2)}\sin^2\theta}{3}$$

$$F_{12} = F_{21} = \frac{1}{6}\left(JZ_1 - \frac{\omega\phi_1}{4}\right) + \frac{\omega}{8}\phi_1\cos 2\theta$$

$$F_{22} = -\frac{1}{24}\left(JZ_1 - \frac{\omega\phi_1}{4}\right) + \frac{\omega}{8}\left(2\phi_0 + \frac{\phi_1}{4}\right)\cos 2\theta - \frac{D_2^{(2)}\cos^2\theta}{3} + \frac{D_2^{(2)}\sin^2\theta}{3}$$

$$G_{11} = G_{22} = 0$$

$$G_{12} = G_{21} = -\frac{1}{8} \left( JZ_1 - \frac{\omega\phi_1}{4} \right) + \frac{3\omega}{32} \phi_1 \cos 2\theta$$

From equation 3,

$$E(\theta) = E_0 + \vec{\alpha} \cdot \vec{\varepsilon} + \frac{1}{2} \vec{\varepsilon} \cdot C \cdot \vec{\varepsilon} + \varepsilon^2 \beta \cdot \vec{\varepsilon} + \varepsilon^3 F \cdot \vec{\varepsilon} + \varepsilon^2 G \varepsilon^2 \quad (4)$$

For the minimum energy of the second order perturbed term [21, 22],

$$\vec{\varepsilon} = -C^+ \cdot \vec{\alpha} \quad (5)$$

Here  $C^+$  is the pseudo inverse of matrix  $C$ , and  $C^+$  can be found using

$$C \cdot C^+ = 1 - \frac{E}{N} \quad (6)$$

Here  $E$  is the matrix with all elements given by  $E_{mn}=1$ .

### 3. Results and discussion:

Because the simulations will be performed for films with two spin layers,  $N = 2$ . From equation 6,

$$C^+_{11} = -C^+_{12} = \frac{C_{22} + C_{21}}{2(C_{11}C_{22} - C_{21}^2)} \text{ and } C^+_{21} = -C^+_{22} = \frac{C_{21} + C_{11}}{2(C_{21}^2 - C_{11}C_{22})}$$

$\varepsilon_1$  and  $\varepsilon_2$  can be found using above equation (5). After substituting  $\varepsilon$  in equation 4, total energy can be found.

$$\text{From equation 5, } \varepsilon_1 = (\alpha_2 - \alpha_1)C^+_{11} \text{ and } \varepsilon_2 = (\alpha_2 - \alpha_1)C^+_{21}$$

$$\varepsilon_1 = 2 \cos \theta \sin \theta (D_2^{(2)} - D_1^{(2)})C^+_{11} \text{ and } \varepsilon_2 = 2 \cos \theta \sin \theta (D_2^{(2)} - D_1^{(2)})C^+_{21}$$

All the simulations will be done for a film which has two different magnetic anisotropy constants

$(D_1^{(2)} \neq D_2^{(2)})$  in two spin layers.

The simulations will be carried out for face centered cubic (fcc) structured ferromagnetic films with two spin layers. For fcc(001) lattice,  $Z_0=4$ ,  $Z_1=4$ ,  $Z_2=0$  and  $\Phi_0 = 9.0336$ ,  $\Phi_1 = 1.4294$  [8-10]. 3-D plot of energy versus angle and spin exchange interaction is given in figure 1. Here other

parameters are fixed at  $\frac{D_1^{(2)}}{\omega} = 100$  and  $\frac{D_2^{(2)}}{\omega} = 5$ . The peaks along the direction of angle are

closely packed compared to second and third order perturbed cases [16, 17, 21, 22, 24]. The cross section of this 3-D plot at one particular angle is given at figure 2. By rotating 3-D plot in figure 1,

figure 2 can be obtained. Energy minimum can be observed at  $\frac{J}{\omega} = 7, 12, 32, 45, \dots$  etc. Energy in

these graphs is in the range of  $10^{13}$ . However, the energy obtained using third order perturbed Heisenberg Hamiltonian was in the range from  $10^{16}$  to  $10^{19}$  [22]. It implies that the energy slightly reduces due to the fourth order perturbation.

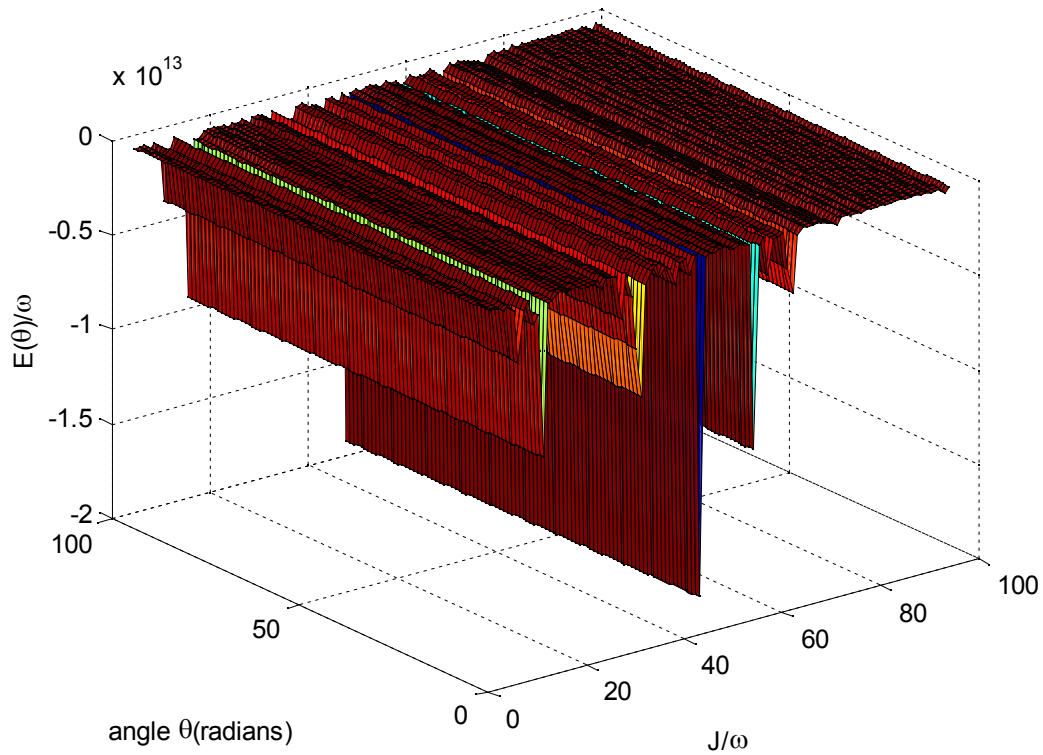


Figure 1: 3-D plot of energy versus angle and spin exchange interaction for  $\frac{D_1^{(2)}}{\omega} = 100$  and  $\frac{D_2^{(2)}}{\omega} = 5$ .

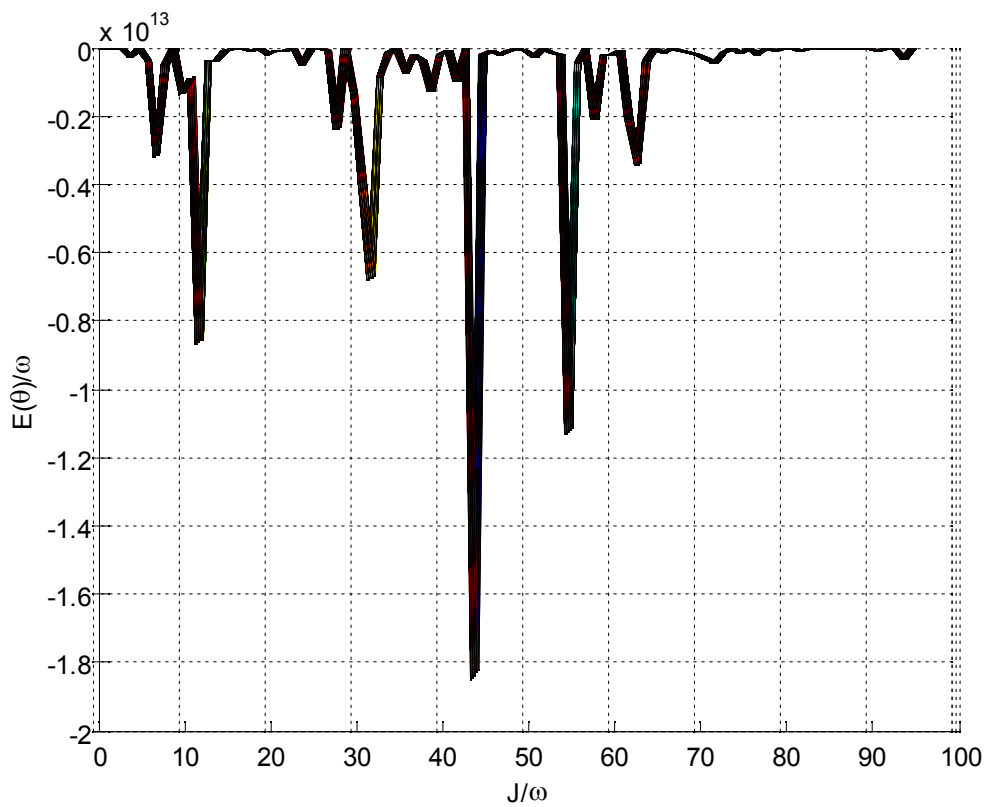


Figure 2: Graph of energy versus spin exchange interaction.

Figure 3 shows the 3-D plot of energy versus angle and spin exchange interaction for  $\frac{D_1^{(2)}}{\omega} = 10000$  and  $\frac{D_2^{(2)}}{\omega} = 5$ . Several peaks can be observed in all the graphs. However, the gap between two peaks is not a constant. The major minimum observed at about  $\frac{J}{\omega} = 45$  in figure 1 has been shifted to about  $\frac{J}{\omega} = 15$  in figure 3. In addition, the magnetic energy increases from  $10^{13}$  to  $10^{30}$  when the value of second order anisotropy constant in bottom spin layer increases. Energy minimum in this case can be observed at  $\frac{J}{\omega} = 8, 15, 33, 38, \dots$  etc. The energy of ferromagnetic thin films found using third order perturbed Heisenberg Hamiltonian was in the range of  $10^{16}$  to  $10^{19}$  [22].

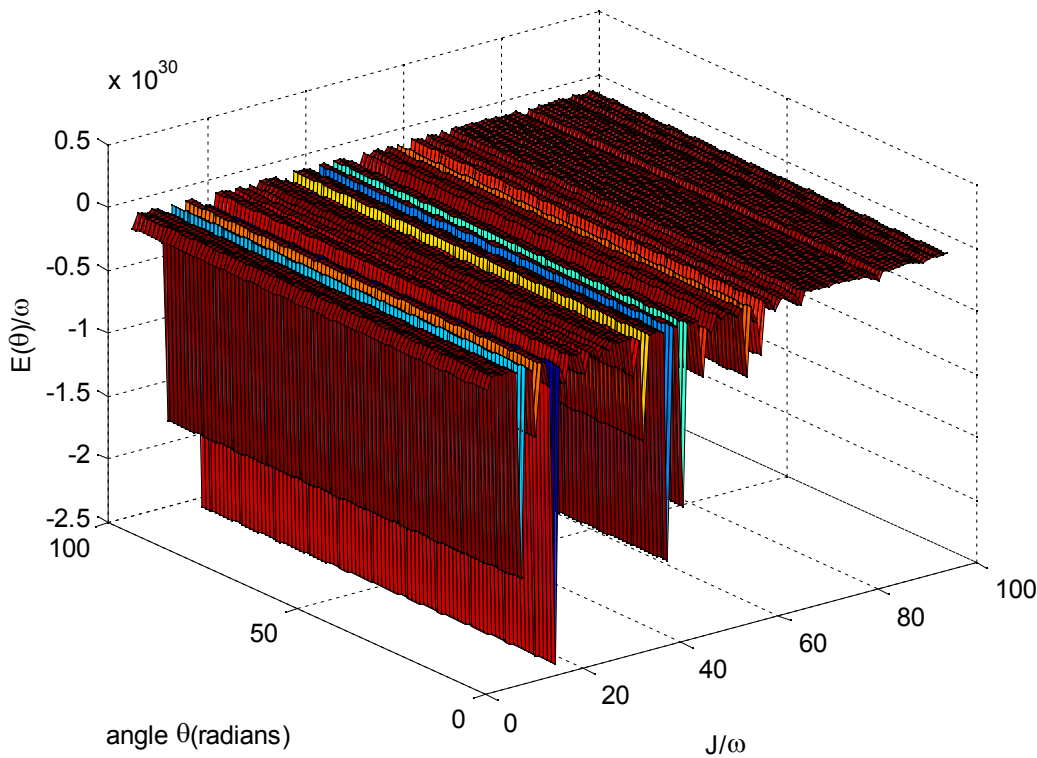


Figure 3: 3-D plot of energy versus angle and spin exchange interaction for  $\frac{D_1^{(2)}}{\omega} = 10000$  and  $\frac{D_2^{(2)}}{\omega} = 5$ .

The 3-D plot of energy versus angle and spin exchange interaction for  $\frac{D_1^{(2)}}{\omega} = 5$  and  $\frac{D_2^{(2)}}{\omega} = 100$  is given in figure 4. The ratios between any two energy parameters are dimensionless. The major energy minima appears at  $\frac{J}{\omega} = 59$  in this case. When second order anisotropy constant in top spin layer is higher than that of bottom spin layer, the major energy minimum shifts to a higher value of

$\frac{J}{\omega}$ . However, the magnetic energy does not change considerably when the second order anisotropy constants of two spin layers are switched as given in figures 1 and 4. Energy minima can be observed at  $\frac{J}{\omega} = 8, 22, 27, 36, 39, 59, \dots$  etc.

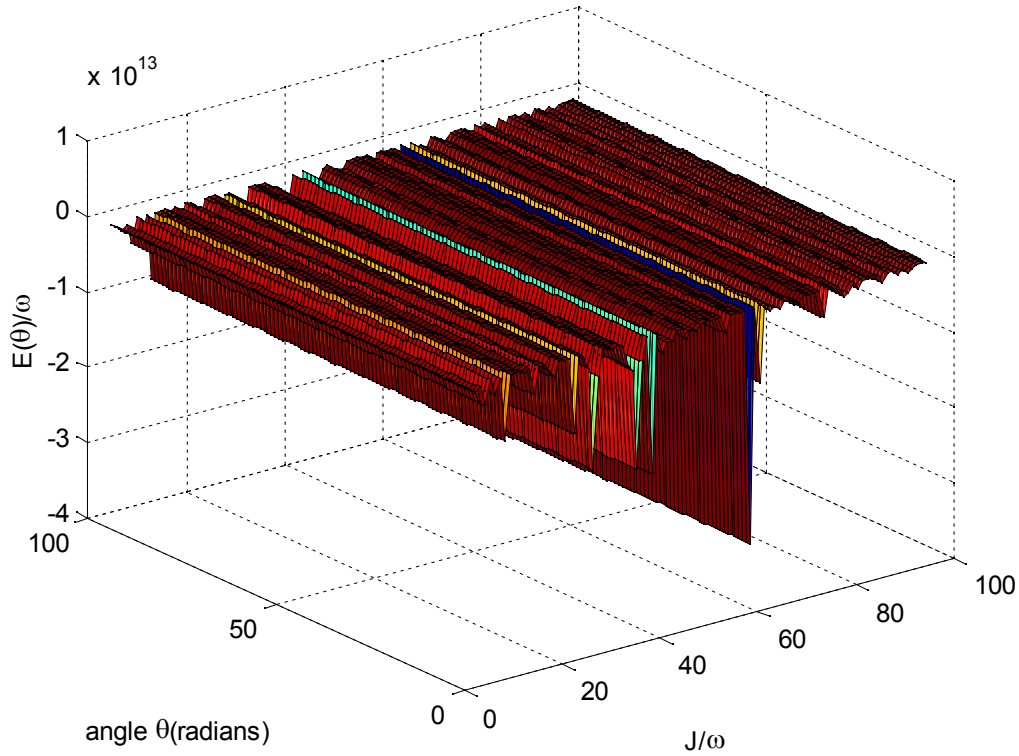


Figure 4: 3-D plot of energy versus angle and spin exchange interaction for  $\frac{D_1^{(2)}}{\omega} = 5$  and

$$\frac{D_2^{(2)}}{\omega} = 100.$$

Figure 5 represents 3-D plot of energy versus angle and second order anisotropy constant of bottom spin layer. Here other parameters were fixed at  $\frac{D_2^{(2)}}{\omega} = 5$  and  $\frac{J}{\omega} = 10$ . The energy varies in the range of  $10^{25}$  in this case. Energy minima can be observed at  $\frac{D_1^{(2)}}{\omega} = 4, 8, 12, 16, \dots$  etc. Energy peaks along the axis of angle are closely packed. The peaks in the same 3-D graphs plotted using third order perturbed Heisenberg Hamiltonian were widely separated [22].

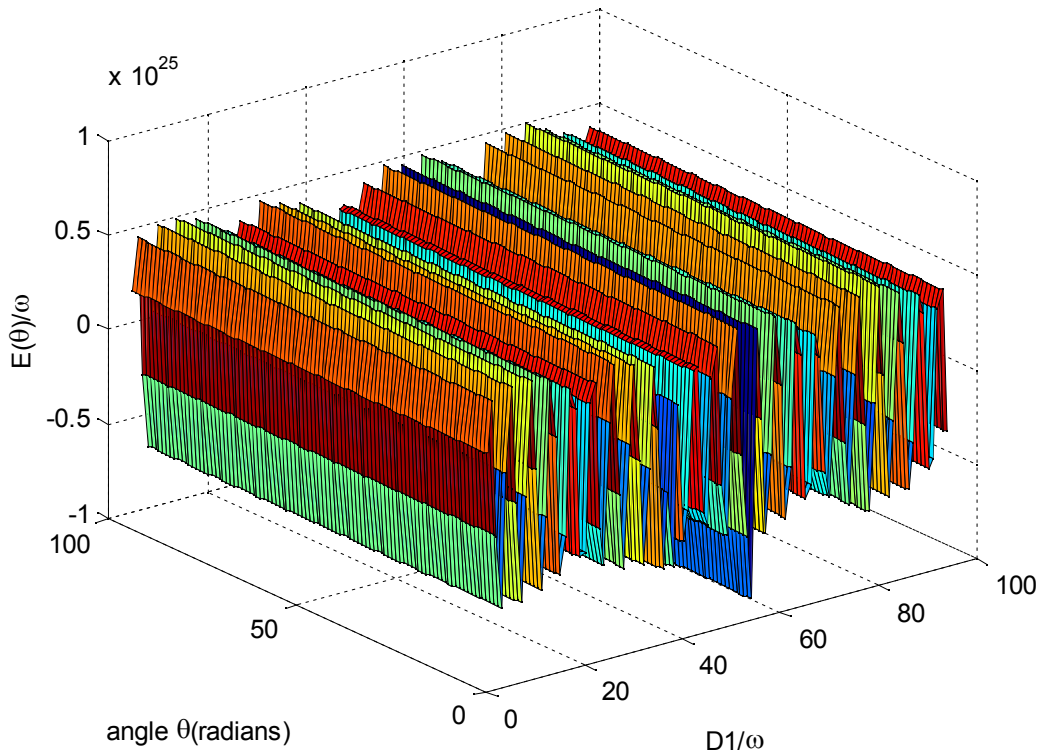


Figure 5: 3-D plot of energy versus angle and second order anisotropy constant of bottom spin layer

$$\text{for } \frac{D_2^{(2)}}{\omega} = 5 \text{ and } \frac{J}{\omega} = 10.$$

Figure 6 represents the 3-D plot of magnetic energy versus angle and second order anisotropy constant of top spin layer. The other values were fixed at  $\frac{J}{\omega} = 10$  and  $\frac{D_1^{(2)}}{\omega} = 10$ . Magnetic energy varies in the range of  $10^{29}$ . Energy minima can be seen at  $\frac{D_2^{(2)}}{\omega} = 6, 9, 14, 18, \dots$  etc.

Energy maxima can be seen at  $\frac{D_2^{(2)}}{\omega} = 3, 8, 12, 16, \dots$  etc. Unlike the previous graphs, the peaks are periodically distributed in this case.

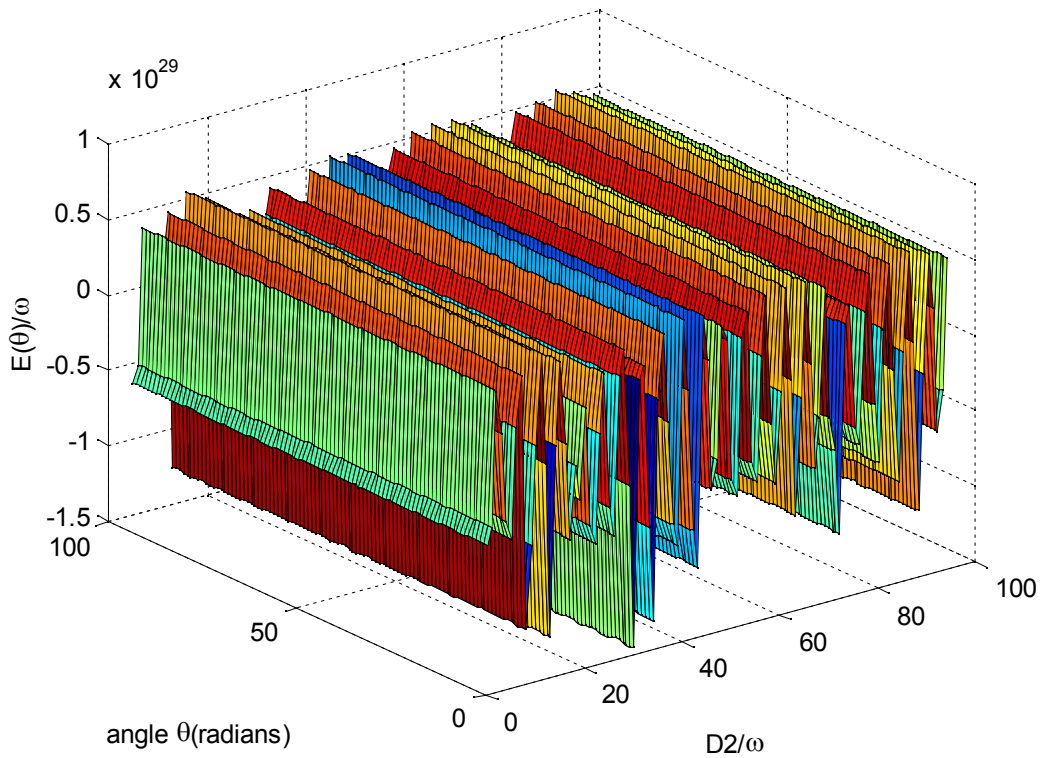


Figure 6: 3-D plot of magnetic energy versus angle and second order anisotropy constant of top spin

layer for  $\frac{J}{\omega} = 10$  and  $\frac{D_1^{(2)}}{\omega} = 10$ .

**4. Conclusion:**

Peaks of all the graphs plotted using fourth order perturbed Heisenberg Hamiltonian are closely packed compared to the graphs plotted using third and second order perturbation Heisenberg Hamiltonian. Adding more terms reduces the space between peaks. Energy minimum can be

observed at  $\frac{J}{\omega} = 7, 12, 32, 45, \dots$  for  $\frac{D_1^{(2)}}{\omega} = 100$  and  $\frac{D_2^{(2)}}{\omega} = 5$ . Energy minimum can be found

at  $\frac{J}{\omega} = 8, 15, 33, 38, \dots$  for  $\frac{D_1^{(2)}}{\omega} = 10000$  and  $\frac{D_2^{(2)}}{\omega} = 5$ . Energy maxima can be seen at

$\frac{D_2^{(2)}}{\omega} = 3, 8, 12, 16, \dots$  for  $\frac{J}{\omega} = 10$  and  $\frac{D_1^{(2)}}{\omega} = 10$ . Peaks are periodically distributed only in one

graph. Although the simulations have been performed for some selected values in this manuscript, the same simulation can be carried out for any values of these energy parameters.

**References:**

1. D. Zhao, Feng Liu, D.L. Huber and M.G. Lagally, *Journal of Applied Physics* (2002), 91(5), 3150.
2. D. Spisak and J. Hafner, *Journal of Magnetism and Magnetic Materials* (2005). 286, 386.
3. Radomska Anna and Balcerzak Tadeusz, *Central European Journal of Physics* (2003), 1(1), 100.
4. C. Cates James and Alexander Jr Chester, *Journal of Applied Physics* (1994), 75, 6754.
5. A. Ernst, M. Lueders, W.M. Temmerman, Z. Szotek and G. Van der Laan, *Journal of Physics: Condensed matter* (2000), 12(26), 5599.
6. Kovachev St and J.M. Wesselinowa, *Journal of Physics: Condensed matter* (2009), 21(22), 225007.
7. Tsai Shan-Ho, D.P. Landau and C. Schulthess Thomas, *Journal of Applied Physics* (2003), 93(10), 8612.
8. A. Hucht and K.D. Usadel, *Physical Review B* (1997), 55, 12309.
9. A. Hucht and K.D. Usadel, *Journal of Magnetism and Magnetic materials* (1999), 203(1), 88.
10. K.D. Usadel and A. Hucht, *Physical Review B* (2002), 66, 024419.
11. U. Nowak, *IEEE transaction on magnetics* (1995), 31(6-2), 4169.
12. M. Dantziger, B. Glinsmann, S. Scheffler, B. Zimmermann and P.J. Jensen, *Physical Review B* (2002), 66, 094416.
13. H. Hegde, P. Samarasekara and F.J. Cadieu, *Journal of Applied Physics* (1994), 75(10), 6640.
14. P. Samarasekara, *Chinese Journal of Physics* (2003), 41(1), 70.
15. P. Samarasekara and F.J. Cadieu, *Chinese Journal of Physics* (2001), 39(6), 635.
16. P. Samarasekara, *Georgian electronic scientific journals: Physics* (2010), 1(3), 46.
17. P. Samarasekara, M.K. Abeyratne and S. Dehipawalage, *Electronic Journal of Theoretical Physics* (2009), 6(20), 345.
18. P. Samarasekara and N.H.P.M. Gunawardhane, *Georgian electronic scientific journals: Physics* (2011), 2(6), 62.
19. P. Samarasekara and Udara Saparamadu, *Georgian electronic scientific journals: Physics* (2012), 1(7), 15.
20. P. Samarasekara and Udara Saparamadu, *Georgian electronic scientific journals: Physics* (2013), 1(9), 10.
21. P. Samarasekara, *Electronic Journal of Theoretical Physics* (2006), 3(11), 71.
22. P. Samarasekara and William A. Mendoza, *Electronic Journal of Theoretical Physics* (2010), 7(24), 197.
23. P. Samarasekara, *Electronic Journal of Theoretical Physics* (2007), 4(15), 187.
24. P. Samarasekara, *Inventi Rapid: Algorithm Journal* (2011), 2(1), 1.
25. F. Viroth, L. Favre, R. Hayn and M.D. Kuzmin, *Journal of Physics D: Applied Physics* (2012), 45, 405003.
26. Y. Laosiritaworn, R. Yimnirun and J. Poulter, *Current Applied Physics* (2006), 6(3), 469.
27. C. Santamaria and H.T. Diep, *Journal of magnetism and magnetic materials* (2000), 212(1-2), 23.
28. V. T. Ngo and H.T. Diep, *Physical Review B* (2007), 75, 035412.
29. J.M. Wesselinowa, *Journal of Physics: Condensed matter* (2006), 18, 8169.